(10) R. L. Dieck and L. Goldfarb, *J. Polym. Sci., Polym. Chem. Ed.*, **15**, 361 (1977).
(11) J. E. White and R. E. Singler, *J. Polym. Sci., Polym. Chem. Ed.*, **15**, 1169 (1977).
(12) H. R. Allcock, T. J. Fuller, D. P. Mack, K. Matsumura, and K. M. Smeltz, *Macromolecules*, **10**, 824 (1977).
(13) J. R. MacCallum and J. Tanner, *J. Macromol. Sci., Chem.*, **A4** (2), 481 (1970).
(14) H. R. Allcock and W. J. Cook, *Macromolecules*, **7**, 284 (1974).
(15) H. R. Allcock, G. Y. Moore, and W. J. Cook, *Macromolecules*, **7**, 571 (1974).
(16) J. K. Valaitis and G. S. Kyker, *J. Appl. Polym. Sci.*, **23**, 765 (1979).
(17) J. R. MacCallum, *Eur. Polym. J.*, **2**, 413 (1966).
(18) C. D. Doyle, *J. Appl. Polym. Sci.*, **5**, 285 (1961).
(19) T. Ozawa, *Bull. Chem. Soc. Jpn.*, **38**, 1881 (1965).
(20) L. Reich, *J. Appl. Polym. Sci.*, **9**, 3033 (1965).
(21) J. H. Flynn and L. A. Wall, *J. Polym. Sci., Polym. Lett. Ed.*, **4**, 323 (1966).
(22) J. H. Flynn and L. A. Wall, *J. Res. Natl. Bur. Stand., Sect. A*, **70**, 487 (1966).
(23) V. S. Papkov and G. L. Slonimskii, *Vysokomol. Soedin., Ser. A*, **10**, 1204 (1968).
(24) H. M. Quackenbos, *Polym. Eng. Sci.*, **6**, 117 (1966).
(25) R. Simha and L. A. Wall, *J. Phys. Chem.*, **56**, 707 (1952).
(26) S. L. Madorsky, *J. Polym. Sci.*, **9**, 133 (1952).
(27) J. E. Clark and H. H. G. Jellinek, *J. Polym. Sci., Part A*, **3**, 1171 (1965).
(28) D. M. Gardner and K. Fraenkel, *J. Am. Chem. Soc.*, **78**, 3279 (1956).
(29) H. R. Allcock, "Phosphorus-Nitrogen Compounds, Cyclic, Linear and High Polymeric Systems", Academic Press, New York, 1972, p 328.
(30) F. G. R. Gimblett, "Inorganic Polymer Chemistry", Butterworths, London, 1963, p 409.
(31) H. H. G. Jellinek, *J. Polym. Sci.*, **4**, 13 (1949).
(32) K. Sebata, J. H. Magill, and Y. C. Alarie, *J. Fire Flammability*, **9**, 50 (1978).
(33) H. R. Allcock, ref 29, p 47.
(34) L. A. Wall and J. H. Flynn, *Rubber Chem. Technol.*, **37**, 937 (1964).

Rotational Relaxation of Chlorobenzene in Poly(methyl methacrylate). 1. Temperature and Concentration Effects

A. C. Ouano*

IBM Research Laboratory, San Jose, California 95193

R. Pecora

Department of Chemistry, Stanford University, Stanford, California 94305.
Received April 10, 1980

ABSTRACT: Rotational motion of chlorobenzene (CB) in poly(methyl methacrylate) (PMMA) over a range of temperature and chlorobenzene concentration is studied by the depolarized dynamic light scattering technique. It was found that the depolarized spectrum of chlorobenzene in PMMA at concentrations of 20 g of chlorobenzene/100 mL or greater shows two widely separated sets of relaxation times, one "fast" on the neat-CB time scale (few picoseconds) and another in the nanosecond and longer time scale (relaxation times typical of macromolecules). The scattered light intensity ratio of the fast to the slow component of the relaxation times was found to increase exponentially with both temperature and concentration. The fast rotational relaxation time was also found to be temperature and CB-concentration dependent.

Introduction

The use of polymers in areas traditionally dominated by steel, glass, and ceramics such as food and electronic-component packaging has continued to grow at an ever-accelerating rate. In this application, the ability of polymeric materials to protect the packaged products from corrosive gases and liquids is of paramount importance. Thus interest in the transport properties of small molecules in amorphous macromolecules has continually intensified in the past 2 or so decades. Scientific studies[1-10] in this area started with the measurement of bulk transport properties, e.g., permeation rates and the diffusivity of gases and liquids in polymers. Although the data obtained by the classical techniques (sorption–desorption measurement) used in the previous studies are very useful, they are also intriguing and often mysterious because they do not follow the relatively simple laws which apply to properties of small-molecule substances. For example, diffusion of gases and liquids in glassy polymers often does not follow Fickian behavior. These complex phenomena arise from the molecular dynamics of the molecules of gases and liquids in polymeric matrices; thus spectroscopic techniques such as NMR[11] and ESR,[12] which are sensitive to molecular dynamics, have been useful in studying them.

A more versatile and perhaps a more powerful technique for studying the motions of molecules in various phases is dynamic light scattering (DLS) photometry. The availability of highly stable lasers has made the rapid development of this technique possible. The book of Berne and Pecora,[13] which offers a comprehensive discussion of the theory and application of this technique, has also contributed in bringing attention to DLS in polymer science.

DLS finds its widest use in the study of the transport properties in liquids. Its application ranges from measurement of center-of-mass diffusion and rotational relaxation of both small molecules and macromolecules in solution[14,15] to the kinetics of polymerization of polystyrene.[16] In this work we used DLS to study the rotational relaxation of chlorobenzene, henceforth referred to as CB, in poly(methyl methacrylate) (PMMA) over a range of temperature and CB concentration.

The CB–PMMA mixture was chosen for this study for the following reasons: (1) CB and methyl methacrylate monomer are miscible in all proportions; (2) CB has a much higher depolarized scattering than PMMA; (3) PMMA and CB are closely matched in refractive index; (4) CB is relatively inert and simply acts as a diluent

0024-9297/80/2213-1167$01.00/0

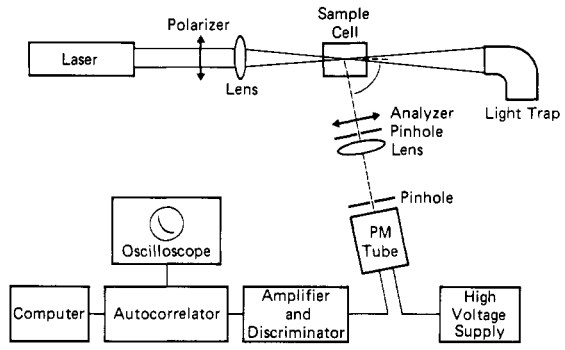

Figure 1. Schematic of typical autocorrelation instrumentation used in this study.

during polymerization of the methyl methacrylate; (5) CB is an important solvent for PMMA in the electronics industry, where PMMA solutions in CB are often used in the manufacture of ultrahigh-density large-scale integrated circuits. PMMA is used to generate extremely small patterns on the order of 2500 Å on silicon chips. In this application, it is essential to understand transport properties of small solvent molecules, such as CB in PMMA.[17]

Instrumentation

The intensity of scattered light depends on the positions and orientations of the scattering entities. If these scatterers are in motion because of thermal energy, for example, the scattering intensity fluctuates. Thus, the measurement of the temporal behavior of these fluctuations can give information on the dynamics, e.g., rotational and center-of-mass diffusions of the scattering entities. Experimentally, the translational diffusion of the scattering species can be obtained by measuring the time autocorrelation function $\langle I_{VV}(0)I_{VV}(t)\rangle$ of the polarized component of the scattered light. If the scattering entities are optically anisotropic, the rotational relaxation can also be obtained from the depolarized autocorrelation function $\langle I_{VH}(0)I_{VH}(t)\rangle$ of the scattered light. This is called the autocorrelation technique and is discussed below.

A. Autocorrelation Technique. Figure 1 shows a schematic of a typical autocorrelation setup. The monochromatic light from the laser is passed through a polarizer which allows only light of the proper polarization (usually vertical) to pass to the focusing lens which focuses the light into the scattering cell. The scattered light intensity is observed at an angle θ, typically 90°, through a set of optical elements and a photomultiplier tube. The signal from the phototube is passed through an amplifier/discriminator before being processed by an *autocorrelator*. What is like a noisy signal ($I(t)$) coming out of the amplifier/discriminator becomes a well-defined function (often an exponential signal) ($\langle I(0)I(t)\rangle$) with a characteristic decay time τ_R after it has been processed by the autocorrelator, as shown in Figure 2. In dilute macromolecular solution, the autocorrelation function can be expressed in terms of the macromolecular center-of-mass translational diffusion constant D and the scattering vector length q

$$\langle I(0)I(t)\rangle = A + B\exp(-2q^2Dt) \qquad (1)$$

where $q = (4\pi/\lambda)\sin(\theta/2)$, A and B are constants, and λ is the wavelength of the light used in the experiment. However, eq 1 is valid only when the product of the scattering vector length and the molecular characteristic length L is equal to or less than unity; otherwise internal motion of the macromolecules will also contribute to the autocorrelation function in eq 1.

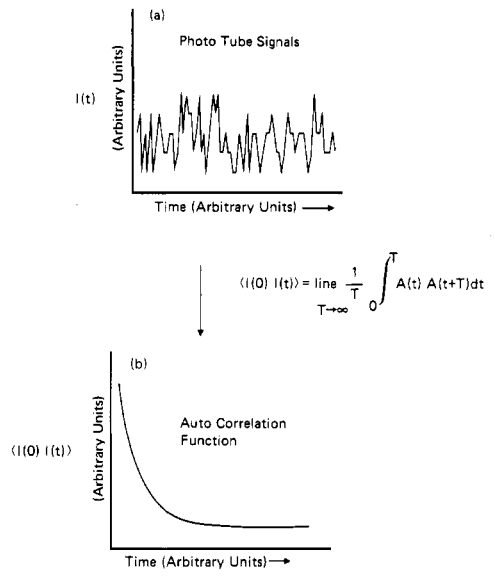

Figure 2. Phototube signal (a) and autocorrelation function (b) of the scattered light from polystyrene latex.

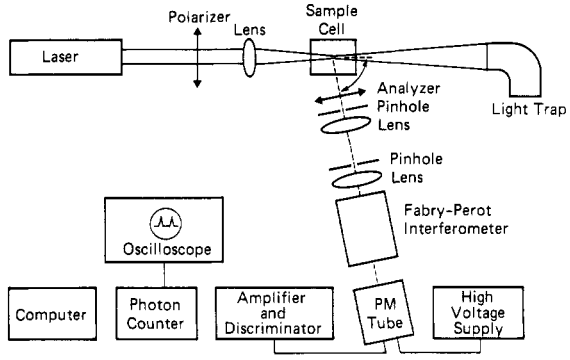

Figure 3. Schematic of a typical Fabry–Perot frequency-scanning instrument as used in this study.

For optically anisotropic molecules in the liquid state the depolarized scattered light autocorrelation function depends on both the translational and the rotational diffusion (D_R) constants

$$\langle I_{VH}(0)I_{VH}(t)\rangle = A + Be^{-(q^2D+6D_R)t} \qquad (2)$$

Because the autocorrelation technique has a limitation on sampling speed of no more than a few megahertz, it is usually limited to the study of rotational diffusion of large molecules in solution or of small molecules undergoing highly hindered rotation, e.g., in systems with very high local viscosity. In ordinary liquids where the rotational time is on the order of picoseconds, the autocorrelation technique is not usable. Consequently, for fast motion, the spectral distribution of the scattered light is measured instead of the autocorrelation function. A Fabry–Perot interferometer is usually used as the frequency-scanning device. This technique is useful for systems which have relaxation times on the nanosecond to few picosecond time scale.

B. Fabry–Perot Spectrometry. Figure 3 shows a schematic diagram of a Fabry–Perot interferometer system. The system is identical with that of the autocorrelation instrument up to the pinhole and focusing lens. After the second pinhole and collimating lens, the light passes through the Fabry–Perot interferometer, which scans the intensity of the scattered light over a free spectral range. The signal from the photomultiplier tube is sent to an amplifier/discriminator before entering a photon

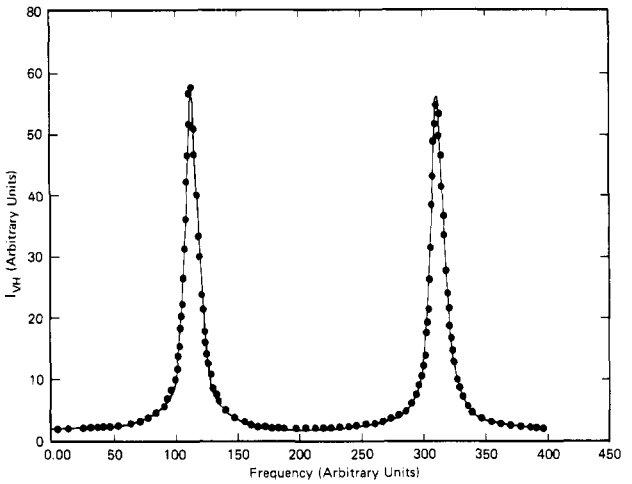

Figure 4. Fabry–Perot spectrum of depolarized scattered light from chlorobenzene at 24 °C.

counter. The number of photons detected per unit time is plotted vs. the frequency and is displayed on an oscilloscope.

The intensity I_{VH} of the depolarized scattered light from a solution of cylindrically symmetric molecules of optical anisotropy β can usually be expressed as a single Lorentzian

$$I_{VH} = A\beta^2 \frac{q^2D + 6D_R}{\omega^2 + (q^2D + 6D_R)^2} \quad (3)$$

where ω is the frequency shift of the scattered light from the incident laser frequency and D_R is the rotational diffusion coefficient. A is an instrumental constant and β is the optical anisotropy of the scattering species. Since the Fabry–Perot technique is only applicable where $6D_R \gtrsim 10^6$ s^{-1} and since $q \sim 10^5$ cm^{-1} (at a scattering angle of 90°) and $D \sim 10^{-6}$ cm^2/s, q^2D can be neglected in eq 3. Thus the rotational diffusion coefficient or the half-width at half-height (hwhh) of the spectrum (see Figure 4) can be calculated by fitting the experimental I_{VH} to

$$I_{VH} = A\beta^2\left(\frac{6D_R}{\omega^2 + 36D_R^2}\right)$$

Experimental Section

A. Sample Preparation. Because of the sensitivity of the quality of light scattering data to the presence of dust and any large inhomogeneity in the sample, we had to develop a proper technique of preparing "dust- and imperfection- (strain-induced microcracks and bubbles) free" samples of CB in PMMA in various concentrations. Obviously, we could not prepare the samples directly from mixtures of PMMA and CB, for even at very high CB concentrations, e.g., 90% CB, the viscosity of high molecular weight PMMA solution is too high to be filtered through a 0.2-μm filter. If the sample is prepared from dilute PMMA solution followed by careful filtration and evaporation, it is difficult or almost impossible to lower the concentration of CB below 20% because of the very slow evaporation rate of CB in this concentration range. For many solvents[12] PMMA becomes glassy at about 30% solvent concentration at room temperature, thus reducing drastically the rate at which the solvent can be removed from the sample. Consequently, the samples containing the range of CB concentrations (0–60 g/100 mL) are best prepared from very clean solutions of CB in methyl methacrylate followed by polymerization to nearly 100% PMMA conversion.

Several techniques of preparing the CB–PMMA samples were tried, but we decided to use the following procedure because it gave us samples with good optical properties for dynamic light scattering experiments. One test of the optical quality of the samples involves the measurement of the Landau–Placzek ratio,

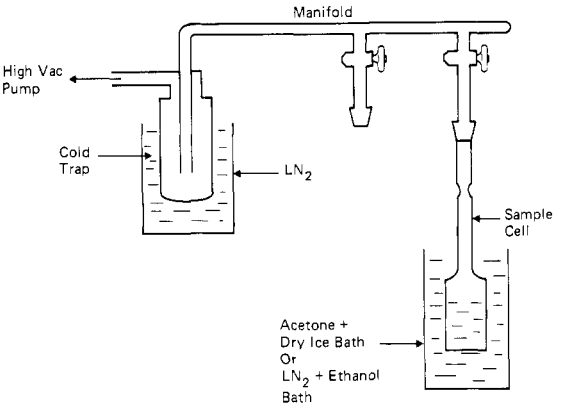

Figure 5. Schematic of the sample degassing system using the "freeze–thaw" technique.

which is the ratio of the central line intensity to the intensity of the Brillouin doublet.[18] A high Landau–Placzek ratio indicates poor sample quality. For example, commercial PMMA samples have ratios of about 20, while our samples all have ratios of less than 10 and most had ratios of about 4.

Clean methyl methacrylate monomer was prepared by vacuum distillation and stored in a septum-sealed flask under an argon atmosphere. Analytical grade CB dried by adding molecular sieve was weighed along with 0.025 g of recrystallized AIBN initiator into a 25-mL volumetric flask to give a range of CB concentrations of 5–60 g/100 mL of solution. The volumetric flask containing the desired amount of CB is filled with the clean methyl methacrylate monomer by using a 20-mL syringe to transfer the methyl methacrylate monomer from the septum-sealed flask. Argon is bled into the septum-sealed flask during the syringe removal of the methyl methacrylate monomer (MMA) to prevent moisture, oxygen, and other impurities from getting into the monomer. The CB and monomer mixture in the 25-mL volumetric flask is placed in a shaker for approximately 1 h. The homogeneous CB–MMA mixture is then filtered into a clean light scattering cell, using a 20-mL syringe fitted with a 0.2-μm Millipore Teflon filter. The light scattering cells used were Hellma 221-QS cells which had been modified to fit our vacuum system (see Figure 5).

After making sure that the CB–MMA mixture in the sample cell was dust-free (this was accomplished by putting the sample in the laser beam and observing the scattering volume through a low-power microscope for the absence of dust particles), we mounted the sample in the vacuum system shown in Figure 5. The sample was then degassed by a "freeze–thaw" technique and sealed under vacuum.

During the "freeze–thaw" operation we noted an interesting phenomenon. Although samples containing 40 g of CB/100 mL of solution and less froze above the −78 °C temperature of the dry ice–acetone mixture, the samples containing 50 and 60 g of CB/100 mL of solution did not. In order to freeze these samples, we had to use a nitrogen–ethanol mixture (ethanol crush) at −120 °C. It should be noted that the freezing points of pure CB and pure methyl methacrylate (−45 and −48 °C, respectively) are well above the dry ice–acetone mixture. Thus there appears to be a large freezing point depression at 50 and 60 g of CB/100 mL of solution.

Immediately upon sealing and allowing the sample to reach room temperature, we obtained its polarized and depolarized spectra by the Fabry–Perot technique. Figure 6 shows a polarized spectrum for a sample containing 20 g of CB/100 mL of solution. The depolarized spectrum of the same sample is shown in Figure 4. From the depolarized spectrum, the CB rotational relaxation time can be calculated.

From the polarized spectrum, the sound velocity may be calculated from the Doppler shift $\Delta\nu$ (see Figure 6) of the Brillouin doublet

$$\Delta\nu = \pm 2n(V_S/C)\nu_0 \sin(\theta/2) \quad (4)$$

where V_S and C are, respectively, the sound and light velocities and n and ν_0 are the refractive index and the frequency of the incident light beam. The Landau–Placzek ratio may also be

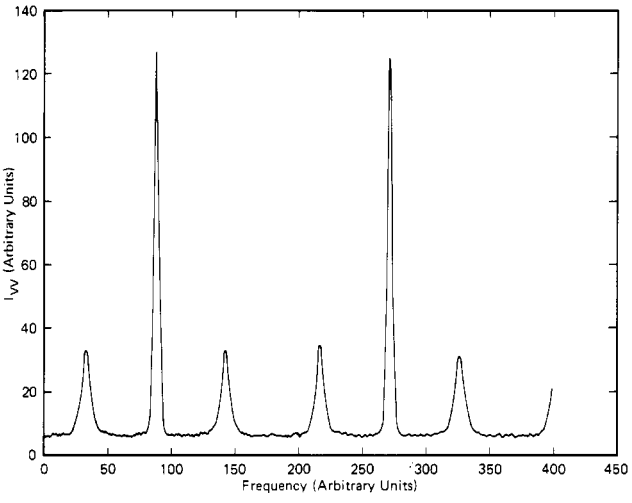

Figure 6. Fabry–Perot spectrum of polarized scattered light from a solution of 20 g of CB/100 mL in methyl methacrylate at 24 °C.

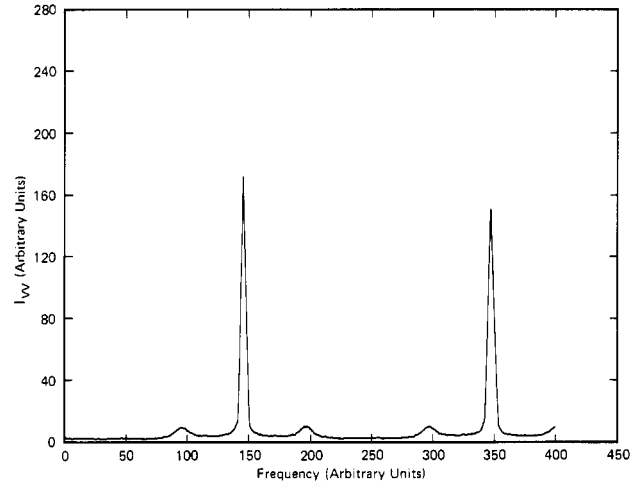

Figure 7. Fabry–Perot spectrum of polarized scattered light from a solution of 20 g of CB/100 mL in PMMA.

obtained from the polarized spectrum.

Polymerization of the samples was initiated thermally by placing them in an oven at 95 °C. After about 3 days the samples usually become very viscous. At this time the temperature was raised to 115 °C and the samples were allowed to continue to polymerize. After about 25 days, the temperature of the samples was gradually lowered to room temperature over a period of about 48 h. This is the most critical period of the sample preparation, for this is the time when bubbles could form, making these useless for light scattering experiments. In spite of the care taken, the volume contraction during polymerization sometimes results in the formation of voids within the sample. In a successful sample, the volume contraction usually manifests itself as a "paraboloid"-like indentation or depression in the sample surface. At room temperature, this indentation is evident in all CB concentrations and is stable for months except at the highest (60 g/100 mL) CB concentration. This suggests a solidlike or at least extremely high macroscopic sample viscosity. Figure 7 shows a polarized spectrum of a sample containing 20 g of CB/100 mL after complete polymerization. The Landau–Placzek ratio for this case is about 4, indicating a very clean sample.

B. Fabry–Perot Spectroscopy. The apparatus used in this study is described in part B of the instrumentation section and the schematic diagram is shown in Figure 3. All of the scattering intensity measurements were done at 90° and the line used was the vertically polarized light of 4880-Å wavelength from a Spectra-Physics Model 165 4-W argon ion laser. The sample holder was thermostated by a Lauda 20R temperature bath, capable of maintaining the sample temperature at ±0.05 °C over a range of temperature 0–95 °C. The frequency-scanning apparatus is a piezoelectrically driven parallel-plate Fabry–Perot interferometer manufactured by Grandt Associates. A similar interferometer is now available commercially from Burleigh Instruments, Inc. The phototube used is an EMI 9558 PMT cooled to −20 °C to lower the dark current. The signal from the phototube is fed to an SSR-1120 photon-counting system which is hard-wired to a Data General Nova Series III computer equipped with a floppy disk data storage system.

The procedure followed in obtaining a spectrum is as follows: The mirrors of the FP spectrometer are adjusted to give a free spectral range of about 100 GHz. The optical elements (beam alignment, pinholes, lenses, and mirrors) are adjusted to obtain the maximum finesse possible (usually about 60). The finesse is usually obtained from the hwhh of the polarized spectrum of a polystyrene standard. As soon as the desired finesse is obtained, the free spectral range is obtained with the sodium D line and/or the Brillouin spectrum of toluene as standard. After the instrument has been properly calibrated, the polarized and depolarized spectra of the sample are taken. If the scattering intensity of the sample is weak (such as for samples containing low CB concentrations), several scans (~20–100) are usually required to obtain a good signal-to-noise ratio. At the end of a certain number of specified scans, the spectrum of the sample is displayed on a CRT. If a spectrum is of sufficiently high quality, as shown in Figure 4, it is stored and copied into a data storage file (a floppy disk in our case) for further analysis.

The spectral fitting program used to analyze our data is capable of fitting the sum of two Lorentzians to the experimental spectra. In cases where two Lorentzians are required to fit the experimental spectra, an estimate of the hwhh of both the narrow and the wide Lorentzians is made for use as an initial "guess" in our fitting program. In addition to the hwhh, the data processing program also gives the relative intensities of each of the Lorentzians as well as the statistical error estimates for the hwhh and the relative intensities. The rotational diffusion constant and the equilibrium constant are then calculated from the hwhh and relative intensities, respectively.

C. Autocorrelation. The apparatus used is described in part A of the instrumentation section and the schematic diagram shown in Figure 1. All of the light scattering intensity measurements were done at 90°, using vertically polarized light of 4880-Å wavelength from a Spectra-Physics Model 165 4-W argon ion laser. The sample holder was thermostated to ±0.05 °C over a range of temperature from 0 to 95 °C. The phototube used was an RCA8575 PMT (thermoelectrically cooled to −30 °C to reduce the dark current), the output of which was fed through an SSR-1120 photon-counting system before being processed by a 48-channel Malvern autocorrelator. The autocorrelator is hard-wired to a Nova Series III computer, where the data can be permanently stored on a floppy disk (random-access data file) or further analyzed.

The procedures followed in obtaining an autocorrelation function of the scattered light from the sample is as follows: After the sample has been equilibrated at the desired temperature, the optical elements are aligned to give the maximum photon count of the scattered light. The autocorrelation sampling rate and the clipping level are set to optimize the quality of the autocorrelation function such that it can be obtained in as short a time as possible. For very weak depolarized scattering experiments, it may take as long as 30 min to obtain a high-quality autocorrelation function. When an autocorrelation function of acceptable quality is obtained, the data are transferred to a Nova Series III computer for further analysis and archieval storage on floppy disk files.

The relaxation times are obtained from the autocorrelation function by fitting eq 2 to the experimental data. Our fitting program is also capable of fitting two exponentials to an experimental autocorrelation function.

Results and Discussion

Concentration Effects. Figure 8 shows the Fabry–Perot spectra of a series of samples over a CB concentration range from 5 to 60 g/100 mL of solution at 60 °C. Spectra of samples containing less than 20 g/100 mL could be represented with a single Lorentzian with a hwhh close to that of the instrumental line width. This indicates the

Table I
Rotational Relaxation Times[a] of CB in PMMA at Various Temperatures and CB Concentrations

CB concn, g/100 mL	1 °C		24 °C		60 °C		95 °C	
	τ_1, ps	τ_2, ns	τ_1, ps	τ_2, ns	τ_1, ps	τ_2, ns	τ_1, ps	τ_2, ns
20	100 ± 10	inst line width	30 ± 5	1.10	8.0 ± 2	0.70	8.0 ± 1	0.15
28	100 ± 10	inst line width	30 ± 5	0.50	8.0 ± 2	0.20	6.0 ± 1	0.10
40	90 ± 10	inst line width	20 ± 2	0.40	10 ± 2	0.40	7.0 ± 1	0.20
50	60 ± 5	inst line width	20 ± 2	0.30	10 ± 2	0.30	7.0 ± 1	0.20
60	20 ± 5	inst line width	20 ± 2	0.30	8.0 ± 1	0.10	7.0 ± 1	0.20
100	10.0 ± 1		8 ± 1		6.0 ± 1		4 ± 1	

[a] τ_1 = fast component of the relaxation-time spectrum. τ_2 = the fastest component of the slow-relaxation-time spectrum.

Table II
Intensity Ratio of the Fast to the Slow Component of the Depolarized Spectra of CB in PMMA

g of CB/100 mL	$K = A_1/A_2$ [a]		
	24 °C	60 °C	95 °C
20	0.40	0.80	0.90
28	0.40	0.80	1.10
40	0.60	1.40	1.60
50	1.20	2.10	2.50
60	2.70	2.75	4.50

[a] Intensity ratio.

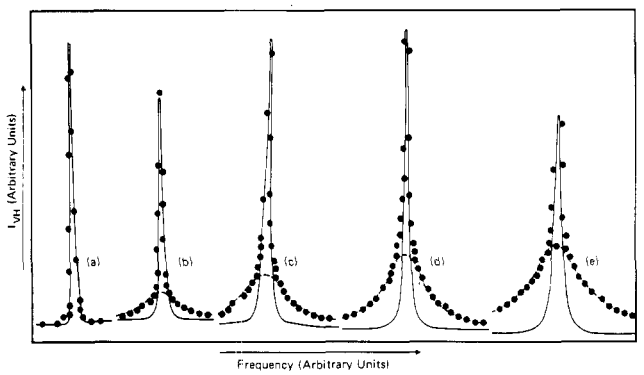

Figure 8. Fabry–Perot spectra of a series of samples of PMMA containing a range of CB concentrations: (a) 5 g/100 mL; (b) 30 g/100 mL; (c) 40 g/100 mL; (d) 50 g/100 mL; (e) 60 g/100 mL.

absence or at best the presence of a very low concentration of CB with relaxation times in the picosecond range. It is also apparent that the samples containing 20 g of CB/100 mL and higher concentration show at least two relaxation times which are sufficiently separated that spectra are best fitted to two Lorentzians.

A Lorentzian fitting routine was used to calculate the relaxation times, and these are listed in Table I. It was found that, while τ_1, the fast component of the spectra, was independent of the free spectral range, τ_2, the slow component of the spectra, was sensitive to the free spectral range used. This indicates that the slow component of the relaxation spectra does not represent a single relaxation time but probably consists of a broad distribution of relaxation times. Thus the τ_2 shown in Table II represent only the fastest components of this distribution which can be sensed at the free spectral range of the experiment. It appears that there are components of the slow relaxation times which are sufficiently slow to be observable in the autocorrelation range, as shown in Figure 9. It is also clear from Figure 9 that the autocorrelation function does not fit a single exponential. It appears that the slow relaxation of CB in PMMA has components with relaxation times longer than several hundred microseconds.

Table I shows that the rotational relaxation time of the fast component, τ_1, is relatively insensitive to the concentration of the CB in PMMA, particularly at the higher temperatures, where it is independent of concentration. However, Figure 8 shows that the intensity of the fast component increases markedly relative to the intensity of the slow component of the spectra. Table II shows the ratio of the intensity of the fast component (A_1) to the intensity of the slow component (A_2) of the spectra for various temperatures and CB concentrations. If we let K be the ratio of A_1 to A_2 and plot the logarithm of K vs. the concentration of CB, we obtain a nonlinear relationship in the temperature range of our experiments, as shown in Figure 10.

It is clear from Figure 10 that the intensity ratio appears to increase more steeply with concentration at 24 °C than at the higher temperatures studied. One possible interpretation of this phenomenon is in terms of free volume. At lower temperatures, where the free volume in the polymer is small, the increase in free volume due to an increase in the CB concentration has a more marked effect in the properties of the polymer than at higher temperatures, where the free volume of the PMMA is already high.

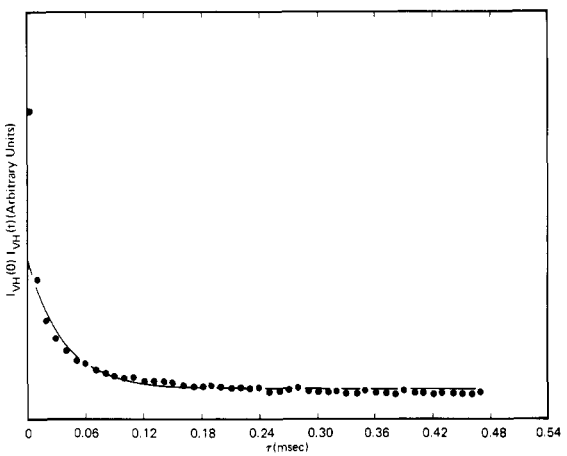

Figure 9. Autocorrelation function of depolarized scattered light from PMMA containing 30 g of CB/100 mL.

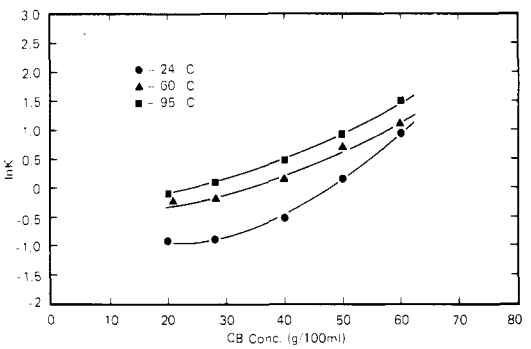

Figure 10. Plot of the logarithm of the equilibrium constant K vs. the CB concentration over a range of temperature.

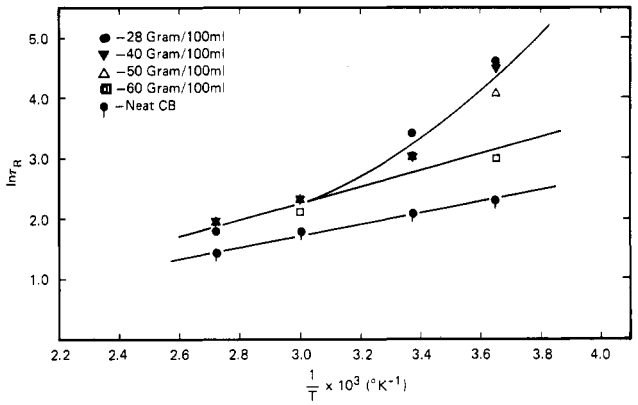

Figure 11. Plot of the logarithm of the relaxation time of the fast component τ_1 vs. the reciprocal of the absolute temperature T.

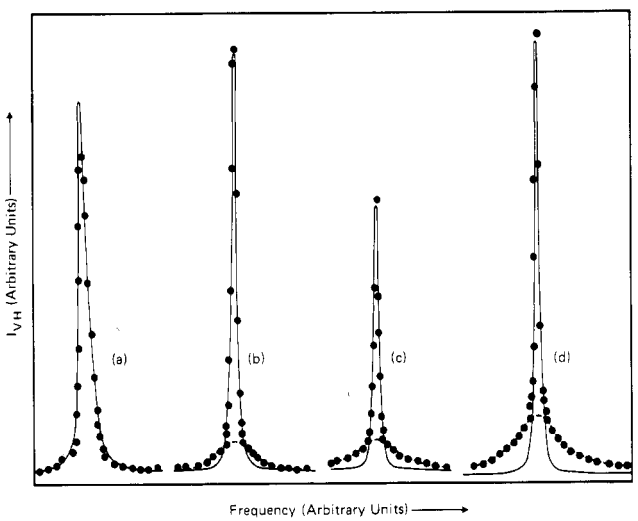

Figure 12. Plot of the Fabry–Perot spectra of the depolarized scattered light from a PMMA sample containing 30 g of CB/100 mL at (a) 1, (b) 24, (c) 60, and (d) 95 °C.

This rationalization of the data in terms of free volume will be dealt with more extensively and quantitatively in part 2 of this work.

Temperature Effects. Table I shows that the fast relaxation time (τ_1) depends significantly on temperature, particularly at the lower CB concentrations and temperatures. If one plots the logarithm of τ_1 vs. the reciprocal of the absolute temperature, one obtains, as might be expected, a linear relationship for neat CB, as shown in Figure 11. However, except for the highest CB concentration, the ln τ_1 vs. reciprocal temperature plot has a nonlinear relationship with a very steep rise in τ_1 at the lower temperatures. This suggests that the activation energy at the lower CB concentrations is strongly temperature dependent. This could be due to the fact that at low concentrations the CB motion is highly hindered by the PMMA and that small changes in temperature (and hence in the PMMA local structure) could have large effects on the CB mobility.

Figure 12 shows Fabry–Perot spectra of a CB–PMMA mixture consisting of 28 g of CB/100 mL over a range of temperature. As in Figure 8, it is evident that the intensity of the fast component of the spectrum increases relative to the slow component as the temperature rises. By plotting the logarithm of the ratio K of the intensities of the fast to the slow component vs. temperature, one obtains a linear relationship, as shown in Figure 13.

One can formulate a model which supposes that CB in PMMA exists in two different environments. In one of these environments, CB can rotate quickly and in the other its rotation is very slow. If the CB in each of the two environments can be imagined to be in "equilibrium", the data of Figure 13 can then be used to obtain the enthalpy difference between CB in these two states. Unfortunately, it is well-known that amorphous solids, particularly glassy polymers, are not in an equilibrium state. Let us, nevertheless, assume that in our samples such an equilibrium exists between the CB which is relaxing fast and that which is undergoing slow reorientation. This is probably a reasonable assumption for well-annealed samples and for those samples which are above T_g, e.g., for the samples at high temperatures and CB concentrations. If we further assume that the concentration of CB is proportional to the intensities of the Fabry–Perot spectra, then K becomes the equilibrium constant between the CB undergoing fast reorientation and the CB in the more highly hindered environment. The derivative of the logarithm of the equilibrium constant K with respect to temperature is related to the enthalpy difference between CB in the two states by the well-known relation

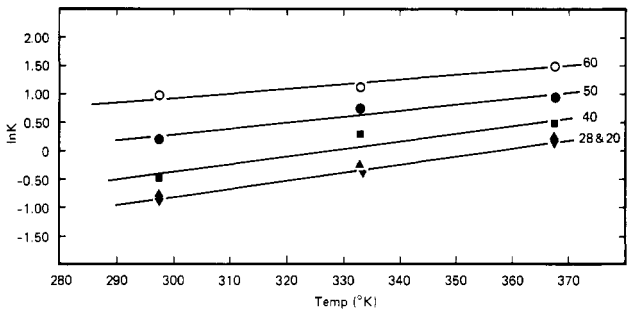

Figure 13. Plot of the logarithm of the equilibrium constant K vs. the absolute temperature T over a range of CB concentrations.

Table III
$\Delta H°$ at Various CB Concentrations

g of CB/100 mL	$\Delta H°$, kcal	g of CB/100 mL	$\Delta H°$, kcal
28	2.4	50	1.8
40	2.2	60	1.3

$$d(\ln K)/dT = \Delta H°/RT^2 \quad (5)$$

Thus $\Delta H°$ can be calculated from the slope of a log K vs. $1/T$ plot and eq 5. The values of the $\Delta H°$ for the different concentrations of CB at 24 °C are given in Table III. Although it is clear that the values of $\Delta H°$ do not change by a large amount with CB concentration, it is also apparent that the $\Delta H°$ decrease with increasing CB concentration, indicating the enthalpy differences between CB in the highly hindered and the freer environment decrease as the CB concentration increases or as the T_g decreases.

Summary

There is strong experimental evidence here that CB in PMMA exhibits at least two relaxation times which are separated by at least 1 order of magnitude in time scale. The fast component has a relaxation time on the order of neat CB and, depending on CB concentration and temperature, it ranges from 7 to 100 ps. There is evidence that the slow component of the relaxation spectrum consists of a broad distribution of relaxation times, extending from nanoseconds to as long as milliseconds in time scale.

The results presented here might be used to provide some information on the nature of the environment of the CB in PMMA. The problem lies in finding a suitable model or models to interpret the complex motion of the CB molecule in the PMMA matrix which gives rise to

spectra of at least two Lorentzians. The fast component of the relaxation spectra exhibits a relaxation time of at most 1 order of magnitude longer than that of neat CB, even though the viscosity of the PMMA matrix is several orders (at least 10 orders) of magnitude higher than that of CB liquid. On the other hand, the slow component shows relaxation times expected of CB in a highly viscous medium.

One possible interpretation of these facts, as mentioned above, is that the CB exists in two types of environments. One type of environment is a characteristic of the neat CB and the other a characteristic of a high molecular weight polymer. In another possible interpretation, we can think of the CB molecules as undergoing two types of motion: (1) the CB molecule could be rotating rapidly but with a restricted angular displacement, e.g., rotating in a conelike volume element and (2) the walls of the cone (the polymer segments) could relax, allowing the CB molecule to undergo cooperative motion with the polymer segment, resulting in a slowly relaxing component. This slow motion of the CB therefore reflects the motion of the polymer chains. Thus these two points of view could be a starting point in building a theoretical interpretation of the motions of CB molecules in PMMA. Part 2 of this work will deal with the theoretical interpretation of the data presented here.

Acknowledgment. We thank Dr. George Heller of the Stanford Research Institute for supplying the vacuum-distilled methyl methacrylate monomer, Mr. Edward Gipstein for the use of his high-vacuum septum, and Dr. Stephen Michelsen for assisting us in setting up the Fabry–Perot spectrometer.

References and Notes

(1) Fugita, H. *J. Phys. Soc. Jpn.* **1953**, *8*, 271.
(2) Fugita, H. *Fortsch. Hoch. Polym. Forsch.* **1961**, *3*, 1.
(3) Fugita, H.; Kishimoto, A. *J. Chem. Phys.* **1961**, *34*, 393.
(4) Kokes, R. J.; Long, F. A.; Hoard, J. C. *J. Chem. Phys.* **1952**, *20*, 1711.
(5) Frisch, H. L. *J. Phys. Chem.* **1957**, *61*, 93.
(6) Meares, P. *J. Polym. Sci.* **1958**, *27*, 391.
(7) Rogers, C. E.; Stannett, V.; Szwarc, M. *J. Polym. Sci.* **1960**, *45*, 61.
(8) Vrentas, J. S.; Duda, J. L. *J. Polym. Sci., Polym. Phys. Ed.* **1977**, *15*, 403.
(9) Paul, D. R. *Ber. Bunsenges. Phys. Chem.* **1979**, *83*, 294.
(10) Cohen, M. H.; Turnbull, D. *J. Chem. Phys.* **1959**, *31*, 1164.
(11) Powles, J. G.; Neale, D. J. *Proc. Phys. Soc., London* **1961**, *77*, 737.
(12) Veksli, Z.; Miller, W. G. *Macromolecules* **1977**, *10*, 686.
(13) Berne, B. J.; Pecora, R. "Dynamic Light Scattering"; Wiley: New York, 1976.
(14) Bauer, D. R.; Brauman, J. L.; Pecora, R. *J. Am. Chem. Soc.* **1974**, *96*, 6840.
(15) Bauer, D. R.; Brauman, J. L.; Pecora, R. *Macromolecules* **1975**, *8*, 433.
(16) Alms, G. R.; Patterson, J. D.; Stevens, J. R. *J. Chim. Phys.* **1979**, *70*, 2145.
(17) Ouano, A. C. *Polym. Eng. Sci.* **1978**, *18*, 306.
(18) Mitchell, R. S.; Guillet, J. E. *J. Polym. Sci., Polym. Phys. Ed.* **1974**, *12*, 713.
(19) Wang, C. C.; Pecora, R. *J. Chem. Phys.*, in press.

Rotational Relaxation of Chlorobenzene in Poly(methyl methacrylate). 2. Theoretical Interpretation

A. C. Ouano*

IBM Research Laboratory, San Jose, California 95193

R. Pecora

Department of Chemistry, Stanford University, Stanford, California 94305.
Received April 10, 1980

ABSTRACT: The depolarized Fabry–Perot spectrum of chlorobenzene (CB) in poly(methyl methacrylate) (PMMA), which exhibits fast (picosecond time scale) and slow, broad-distribution (nanosecond to millisecond) relaxation times, is interpreted in terms of two theories, the "diffusion in two environments" (DITE) theory and the restricted rotational diffusion (RRD) theory. The DITE theory along with the free-volume theory was used to estimate the critical void volume per CB molecule, which allows fast relaxation, as 203 Å^3. The RRD theory was used to calculate the cone angle of rotation as well as the rotational diffusion coefficient over a range of temperature and CB concentrations.

Introduction

In part 1 of this work (see preceding paper), we reported experimental results on the dependence of the rotational relaxation of chlorobenzene (henceforth designated as CB) in poly(methyl methacrylate) (henceforth designated as PMMA) on temperature and CB concentration. We found that the Fabry–Perot spectra of CB–PMMA samples having CB concentrations equal to and greater than 20 g of CB/100 mL of the CB–PMMA mixture could best be fit to two Lorentzians, as in Figure 1, indicating that there exist at least two relaxation times which are widely separated in time scale. The wide Lorentzian, representing the fast component, is in the picosecond time scale and appears to be independent of the free spectral range (FSR), thus indicating it to have a single relaxation time or a very narrow relaxation time distribution. The half-width at half-height (hwhh) of the narrow Lorentzian, however, appears to change with the FSR, suggesting that it consists of a wide distribution of relaxation times having components detectable in the autocorrelation time scale, i.e., microseconds or longer.

In this work we propose that the results presented in part 1 can be interpreted in terms of two well-known theories: the "diffusion in two environments" (DITE) theory[1] and the "restricted rotational diffusion" (RRD) theory.[2] These theories have been used to explain the dielectric behavior of molecules trapped in matrices.[1,2] In these systems it has been observed that the dipolar auto-

0024-9297/80/2213-1173$01.00/0